Microbial Ecology (2021) 81:941–953
https://doi.org/10.1007/s00248-020-01673-9

ENVIRONMENTAL MICROBIOLOGY

Phosphate-Arsenic Interactions in Halophilic Microorganisms of the Microbial Mat from Laguna Tebenquiche: from the Microenvironment to the Genomes

L. A. Saona[1,2] · M. Soria[1] · V. Durán-Toro[3] · L. Wörmer[4] · J. Milucka[2] · E. Castro-Nallar[5] · C. Meneses[6] · M. Contreras[7] · M. E. Farías[1]

Received: 1 October 2020 / Accepted: 22 December 2020 / Published online: 2 January 2021

Abstract

Arsenic (As) is a metalloid present in the earth's crust and widely distributed in the environment. Due to its high concentrations in the Andean valleys and its chemical similarity with phosphorus (P), its biological role in Andean Microbial Ecosystems (AMEs) has begun to be studied. The AMEs are home to extremophilic microbial communities that form microbial mats, evaporites, and microbialites inhabiting Andean lakes, puquios, or salt flats. In this work, we characterize the biological role of As and the effect of phosphate in AMEs from the Laguna Tebenquiche (Atacama Desert, Chile). Using micro X-ray fluorescence, the distribution of As in microbial mat samples was mapped. Taxonomic and inferred functional profiles were obtained from enriched cultures of microbial mats incubated under As stress and different phosphate conditions. Additionally, representative microorganisms highly resistant to As and able to grow under low phosphate concentration were isolated and studied physiologically. Finally, the genomes of the isolated *Salicola* sp. and *Halorubrum* sp. were sequenced to analyze genes related to both phosphate metabolism and As resistance. The results revealed As as a key component of the microbial mat ecosystem: (i) As was distributed across all sections of the microbial mat and represented a significant weight percentage of the mat (0.17 %) in comparison with P (0.40%); (ii) Low phosphate concentration drastically changed the microbial community in microbial mat samples incubated under high salinity and high As concentrations; (iii) Archaea and Bacteria isolated from the microbial mat were highly resistant to arsenate (up to 500 mM), even under low phosphate concentration; (iv) The genomes of the two isolates were predicted to contain key genes in As metabolism (*aioAB* and *arsC*/*acr3*) and the genes predicted to encode the phosphate-specific transport operon (*pstSCAB-phoU*) are next to the *arsC* gene, suggesting a functional relationship between these two elements.

Keywords AMEs · Arsenic · Phosphate · Microbial mat · *arsC* · *pstSCAB-phoU*

Introduction

Low oxygen pressure, high UV radiation, constant volcanic eruptions, high thermal fluctuation, and extreme aridity, among other conditions, make the Atacama Desert one of the most extreme environments in the world [1–5]. Hyperaridity is one of the main characteristics differentiating the Atacama Desert from other extreme environments. The

✉ L. A. Saona
saona.luis.a@gmail.com

✉ M. E. Farías
mefarias2009@gmail.com

[1] Laboratorio de Investigaciones Microbiológicas de Lagunas Andinas (LIMLA), Planta Piloto de Procesos Industriales Microbiológicos (PROIMI), CCT, CONICET, San Miguel de Tucumán, Tucumán, Argentina

[2] Department of Biogeochemistry, Max Planck Institute for Marine Microbiology, Celsiusstrasse 1, 28359 Bremen, Germany

[3] Hydrothermal Geomicrobiology Group, MARUM Center for Marine Environmental Sciences, University of Bremen, Bremen, Germany

[4] Organic Geochemistry Group, MARUM—Center for Marine Environmental Sciences, University of Bremen, Leobener Str. 8, 28359 Bremen, Germany

[5] Facultad de Ciencias de la Vida, Center for Bioinformatics and Integrative Biology, Universidad Andres Bello, Santiago, Chile

[6] Centro de Biotecnología Vegetal (CBV), FONDAP Center for Genome Regulation, Universidad Andres Bello, Santiago, Chile

[7] Centro de Ecología Aplicada, Santiago, Chile

characteristic dryness of the region is attributed to its subtropical location, where the climate has remained unchanged for more than 150 million years [5–7]. Because of this, the Atacama Desert is the oldest continuously arid desert on the planet Earth. However, the Atacama Desert also hosts many Andean lakes, which have been characterized mostly by alkaline pH, high salinity, and high concentrations of metals and metalloids from volcanic activity, specifically arsenic (As) [8–11]. In Andean lakes, different kinds of extremophilic microbial communities, denoted as Andean Microbial Ecosystems (AMEs), have been discovered and characterized in recent years [10, 12–17]. The physicochemical characteristics of current Andean lakes make them excellent natural laboratories for the investigation of AMEs' adaptation to high As concentrations under different phosphate concentrations.

Since As is an extremely deleterious element for cells, microorganisms have evolved specific mechanisms to cope with its toxicity, such as extracellular As precipitation, chelation, intracellular sequestration, active extrusion, or biochemical transformation (by redox processes or methylation) [18]. Nonetheless, some microorganisms can use this metalloid as an energy source [19, 20] and play a role in its biogeochemical cycle [21]. For instance, the microbial mats of Laguna Brava, also located in the Salar de Atacama, can incorporate As into exopolysaccharides (EPS), having a direct impact on As mobility and therefore on the As cycle in the lake [22]. In Laguna Diamante, located in the crater of the Galán volcano (Argentina), up to 300 mg/L of As were detected in summer [16]. On the volcanic rocks present in the lake, biofilms composed of 94% by archaeal family Halobacteriaceae have been described [20]. Metagenomic studies revealed that genes related to As metabolism were abundant and diverse in these biofilms and also in *Halorubrum* sp., especially those related to the use of As as a source of energy i.e. *aioAB* and *arrAB* [16, 20]. The presence of these genes suggested that microorganisms present in the biofilms could have the ability to metabolize As in order to obtain energy. Furthermore, *Halorubrum* DM2 sp. isolated from these biofilm samples was shown to increase its growth rate in the presence of As and to have a higher level of *aio* and *arr* gene expression in the presence of As [19].

One of the most relevant characteristics of As and its relationship with biological systems is the chemical similarity with the element phosphorus (P). These are considered chemical analogs since they share characteristics such as atomic radii and identical states of electronegativity and oxidation [23]. In their most prevalent oxidized forms, arsenate (AsO_4^{3-}) and phosphate (PO_4^{3-}), both species are negatively charged at physiological pH. In fact, both molecules have similar speciation at the respective pH and similar pKa values [23–26]. Based on these similarities, As can enter the cells through phosphate transporters (Pst and Pit) and display its harmful effects on different cellular mechanisms and components [27, 28]. Understanding the relationship between As and P would help us comprehend the beginning of life at 4 billion years ago, where primordial biochemical processes started [29, 30]. It is presumed that As may have had a key role as a substrate for an ancestral arsenite oxidase enzyme in As-based metabolisms [31–33] and been associated with the precipitation of carbonates by biological activity in fossil stromatolites 2.7 billion years ago [29], a geological period during which phosphate would not have been available for metabolic activity [34, 35]. Phosphate is geochemically scarce and difficult to access, because it is complexed to rocks and minerals. Its use requires enzymatic mechanics that is hypothesized not to have been present in early metabolisms [36].

Most studies have focused on As resistance and metabolism in AMEs and microbial isolates [10, 19, 37–40]. However, little is known about the influence of phosphate concentration on the biological effect of As. In order to address this question, we investigated the microbial mats present in Laguna Tebenquiche in the Atacama Desert. This lake is located in the center of the Salar de Atacama and is one of the largest water bodies present in the area. Although the As concentration in the water column is lower than in other lakes (0.053 mM), it is 4.8 times higher than the total P concentration (0.011 mM) in situ [10, 41], a characteristic that does not occur in other Andean lakes (Laguna Diamante, Laguna La Brava, Laguna Socompa) where the P concentration is always bigger than the As concentration [41]. This makes the microbial mats inhabiting Laguna Tebenquiche—composed mainly of Proteobacteria and Bacteroidetes [41]—an optimum model to study the metabolism related to As under low phosphate concentrations.

Previously, we outlined the hypothesis that phosphate concentration could have an effect on the presence of genes related to As metabolism and thus on the microbial diversity of an ecosystem [41]. Here, we report a study of the biological role of As in the Laguna Tebenquiche microbial mat, asking whether low P concentration affects As metabolism, and if a relationship between As and P can be detected in this extremophile ecosystem. We determined the distribution of As in the microbial mat. Additionally, we aimed to reveal which taxa from the microbial mat were better adapted to tolerate As when phosphate concentration is low, and to what degree isolated microorganisms were resistant to As when grown with only trace phosphate concentrations. Finally, we aimed to identify the key genes related to As metabolism in the isolates and whether they are linked to phosphate-related genes.

Methods

Sampling Site

Laguna Tebenquiche is located in Antofagasta, Chile, near the central area of the Salar de Atacama (S 23° 08′ 18.5″ W 68° 14′ 49.9″), and it is one of the largest water bodies in this

system [10]. Organisms in this lake are subjected to stress conditions such as high UV radiation, high thermal oscillation (day-night), high salinity, and presence of heavy metals due to volcanic activity, among others [10, 42, 43]. The organic-rich microbial mat [10] inhabiting this lake was submersed in ca. 5 to 15 cm of water and was very gelatinous, containing only a few trapped mineral particles. In November 2016, microbial mat was collected in sterile environmental sampling bottles. A part of the sample was directly frozen and later used for the μ-XRF (see below). Another part of the mat was used to obtain enrichment cultures and isolates. For this last purpose, the subsamples were stored at 4 °C and processed a week later in the laboratory, as described below.

Elemental Mapping with μ-X-ray Fluorescence

A microbial mat slice of 10-mm thickness was obtained using a Leica CM 1900 Cryostat at Max Planck Institute for Marine Microbiology (Fig. 1). Elemental mapping of the slice was performed on a M4 Tornado system (Bruker Nano Analytics) equipped with a micro-focused Rh source (50 kV, 600 μA) with a poly-capillary optic (20-μm spot size). Measurements were conducted under vacuum (19.9 mbar), with a pixel size of 50 μm, a scan time of 30 ms per pixel and 2 scans per pixel. The analyzed area of the mat section had a size of 4.0 × 10.3 mm^2 (16,480 pixels). Data were initially processed and visualized with M4 Tornado Software version 1.3. The *xy*-matrices of individual elements were afterward imported into Matlab (R2016b) and plotted together with a high-resolution picture of the mat slice by referencing three teaching points.

Enrichment Cultures and Isolation of Halophilic Strains from Laguna Tebenquiche Microbial Mats

Enrichment cultures were obtained in 250-mL Erlenmeyer flasks with 60 mL of chemically defined medium (CDM) [44] supplemented with sodium arsenate dibasic heptahydrate 25 mM ($Na_2HAsO_4 \cdot 7H_2O$) and inoculated with 5 g of a microbial mat from the Laguna Tebenquiche. To analyze which taxa are selected in low phosphate concentration, CDM medium was modified from its original composition using 0 and 1 mM of K_2HPO_4 as the unique added source of phosphate. The salinity of the Laguna Tebenquiche varies between 1 and 30% (w/v) depending on the time of year (due to the cycles of evaporation and precipitation) and also depending on the area of the lake [15]. Based on this, both phosphate conditions were repeated using CDM medium supplemented with 15% and 25% NaCl to emulate the high salinity (NaCl) of Laguna Tebenquiche. The summary of all different conditions is shown in Table S1.

To enrich for and isolate halophiles able to grow at low P and high As concentrations, flasks containing 2 g of microbial mat and 20 mL of CDM with 20% NaCl, 25 mM As(V), and no added of phosphate were incubated at 37 °C for 7 days with stirring at 120 rpm. In order to avoid pH variations because of As presence or microbial growth, the CDM was buffered at pH 7.5 with 5 mM Tris-HCl. The enrichments were streaked onto plates with CDM medium supplemented with 20% NaCl containing 25 mM As(V) without phosphate addition. After 5 days of incubation of plates at 37 °C, two types of colonies were observed that differed mainly in color. The two well-isolated colonies were restreaked several times at enrichment temperatures to ensure axenic cultures.

Growth Curves and Minimum Inhibitory Concentration

Standard growth curves were constructed in CDM liquid medium supplemented with 20% NaCl by using 0 and 1 mM of K_2HPO_4 and different As(V) concentrations: 25, 50, and 100 mM.

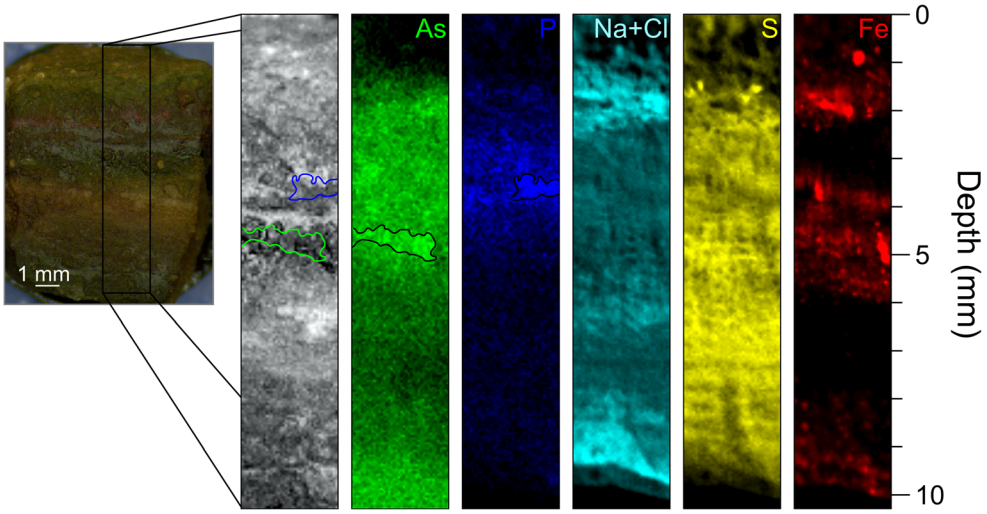

Fig. 1 Micro X-ray fluorescence (μXRF) elemental maps showing relative abundances of As, P, Na+Cl, S, and Fe together with a photographic image of the analyzed slice of the microbial mat from Laguna Tebenquiche

The minimum inhibitory concentration (MIC) assays were performed by using solutions containing 500 mM As(V) prepared in 300 μl CDM medium (500 mM was the maximum concentration tested). Serial dilutions were set in 96-well microplates and inoculated with 5 μL of microbial cultures (archaeon and bacterium) grown up to OD_{600}~0.05. Microplates were incubated at 37 °C and microbial growth was assessed after 72 h. For the analysis of the results, OD_{600} readings of each well were made using the negative control (culture medium without inoculation) as a blank, where any reading with a difference ≤ 5% with the blank was considered growth inhibition. Isolates grew even in the highest concentration of arsenate; therefore, no MIC was obtained. No precipitates were observed in the culture supplemented with 500 mM of arsenate and the pH did not vary.

High-Throughput DNA Sequencing

To generate taxonomic profiles of the enrichment cultures, total DNA was obtained from 2 mL of microbial enrichments after 7, 15, and 30 days of growth. The supernatant of each sample was separated by centrifugation at 10,000*g*. The pellet was used for DNA extraction using the FastDNA SPIN Kit for Soil (MP Biomedicals, Inc.) according to the manufacturer's protocol. The DNA was sent to Macrogen, Inc. (Seoul, Republic of Korea) where amplicons of the region V3-V4 for 16S rRNA genes were generated with primers Bakt-341F and Bakt-805R [45]. Amplicon libraries were sequenced using the Illumina MiSeq platform at Macrogen. The total numbers of raw data are shown in Table S1.

To sequence the microbial isolates (16S rRNA gene and whole genome), total DNA was obtained from the isolated strains grown in CDM medium in the exponential phase. The extraction of the genomic DNA was performed using the FastDNA SPIN kit (MP Biomedicals, Inc.) following the protocol supplied by the manufacturer.

In order to identify the genus of the isolates, the partial 16S rRNA gene was amplified by PCR using two pairs of primers. To identify archaea, the F344 (5′-ACG GGG YGC AGC AGG CGC GA-3′) and R915 (5′-GTG CTC CCC CGC CAA TTC CT-3′) were used [19, 46]. Samples were denatured at 94 °C for 4 min, and amplification reactions were performed in 30 cycles: denaturation (1 min, 94 °C), primer annealing (1 min, 60 °C), extension (1 min, 72 °C), and a final extension step of 5 min at 72 °C. To identify bacteria, the F27 (5′-AGA GTT TGA TC(A/C) TGG CTC AG-3′) and R1492 (5′-TAC GG(C/T) TAC CTT GTT ACG ACTT-3′) were used [47]. The reaction starts with denaturation at 94 °C for 3 min, and amplification was carried out in 30 cycles: denaturation (45 sec, 94 °C), primer annealing (30 sec, 55 °C) and extension (90 sec, 72 °C), with a final extension step of 10 min at 72 °C. For both pairs of primers, the PCR reaction was carried out in a thermocycler T1 thermoblock (Biometra). The reactions were performed in 50 μL volumes containing 10 μL of 5× buffer, 200 μM each of dNTPs, 250 nmol of each primer (Genbiotech), and 2 U Taq DNA polymerase (Invitrogen) brought to a final volume of 50 μL with Milli-Q water. The PCR products were analyzed in 1% (w/v) agarose gel and stained with SYBR Safe (Invitrogen™). To carry out the clone sequencing, the chain termination method of Sanger, by the DNA analyzer 23ABI Prism 3730XL in Macrogen (Korea), was done. The resulting DNA sequences were compared with the data accessible through NCBI (National Centre for Biotechnology Information) using BLASTn [48].

Whole-genome shotgun sequencing was also done for the two strains isolated from Laguna Tebenquiche (named TLS-6 and TLS-7). Total DNA was obtained as described previously and libraries were prepared as in the Illumina TruSeq protocol. DNA sequencing was carried out in an Illumina MiSeq machine with a 2 × 250 bp layout. Sequence data have been deposited in NCBI under BioProject PRJNA643293.

16S rRNA Amplicon Processing

Raw sequences were analyzed as in DADA2 under default settings [49]. The taxonomic assignments were made through the SILVA database (version 132) [50]. Raw data have been deposited in NCBI under BioProject PRJNA643280.

The quality profiles of the forward and reverse sequences were inspected, and these were filtered with the "filterAndTrim" function. The number of sequences that were retained after each step in the DADA2 pipeline is detailed in the Table S2. The sequences belonging to bacteria and archaea were separated to analyze the similarity between them under different conditions. More detailed information about the processing of the sequences through DADA2 is found in the supplementary material (Table S2). Finally, the remaining sequences were used for taxonomy assignments with the Phyloseq package [51].

Functional Prediction and Visualization

Functional potential prediction of the microbial community was carried out using the PICRUSt2 algorithm [52, 53]. For the analysis, an OTU table (otu_table) together with a table with all the sequences (colnames (otu_table)) was extracted from the phyloseq object. Both tables were used as input files for metagenomic prediction by means of the PICRUSt2 pipeline (picrust_pipeline.py). From the output files generated by PICRUSt2, the normalized table with the number of copies of the 16S rRNA gene was used for functional metagenome prediction according to the Kyoto Encyclopedia of Gene and Genomes (KEGG). The visualization of functional prediction data was performed using the graphic/statistical software STAMP (statistical analysis of taxonomic and functional profiles) version 2.1.3 [54].

The investigated genes related to As metabolism were those belonging to *arsRDABC* operon, which confer high levels of As resistance in a range of bacterial species [18]. In addition, *acr3* has been identified as a widely distributed arsenite efflux pump in AMEs [37, 55]). Additionally, the *aioAB* genes and *arrAB* genes, coding for arsenite oxidase and respiratory arsenate reductase, respectively, were also investigated. Finally, the genes related to phosphate metabolism were also investigated, specifically the *pstSCAB-phoU* genes and *phoB*/*phoR* genes belonging to the Pho regulon.

Statistical Analysis

The alpha diversity indices (observed, Chao1, Shannon, and Simpson) for each sample were calculated using the phyloseq package version 1.30.0 [51] in the R version 3.6.3 software [56]. Community and environmental distances were compared by non-metric multidimensional scaling (NMDS), based on Bray-Curtis distance measurements by means of the *ordinate* function of the phyloseq package using a ntaxa = 696. Importance was determined at the 95% confidence interval ($p = 0.05$).

Results

Elemental Mapping of the Microbial Mat

Organic-rich and non-lithifying microbial mats from the hypersaline Laguna Tebenquiche have a dome-like macroscopic morphology where the typical layers are formed [10]. Elemental mapping using μ-XRF spectroscopy revealed the presence of As in a 10-mm-thick slice of a microbial mat from Laguna Tebenquiche (Fig. 1). As was present along the microbial mat, with an abundance, expressed as weight percentage (0.17%), comparable to elements with known biological roles like Fe (1.45%) and P (0.40%) and other micronutrients like Cu (0.05%) and Mn (0.44%) (Table S3). The highest concentration of As (drawn in Fig. 1) was observed in the upper half, coinciding remarkably with the dark green layer of the microbial mat (Fig. 1). On the other hand, the highest concentration of P was detected also in the upper-middle section of the mat. However, a clear separation between areas of maximum abundances of both elements was observed. Neither As nor P was detected in the top edge of the mat (Fig. 1). Both Na and Cl were abundantly present throughout the section, a result consistent with the high concentration of NaCl in the lake (Fig. 1). Fe was detected in localized areas mainly in the middle of the mat and also on the top and bottom edges, while S was evenly distributed throughout the section (Fig 1).

Microbial Biodiversity of the Microbial Mat Enrichment Cultures

Microbial composition of the enrichment cultures obtained from the microbial mat from Laguna Tebenquiche was investigated using 16S rRNA amplicon sequencing. Between 85,000 and 145,000 raw reads were obtained (per condition) from the microbial mat sample enriched under As stress and different P and NaCl concentrations (Table S2). The NaCl concentration produced significant changes in alpha diversity in all the conditions tested (Fig. 2); the number of observed species (observed), the abundance of unique or rare individuals (Chao1), the dominance (Simpson), and richness and abundance (Shannon) strongly increased at 25% NaCl (Fig. 2). On the other hand, mat samples incubated without added phosphate showed slight increases in the observed and Chao1 indices in both 15% and 25% NaCl. But in terms of both Simpson and Shannon indices, the samples without phosphate addition and 25% NaCl have higher values (Fig. 2). The non-metric multidimensional scaling (NMDS) based on the Bray-Curtis differences between the microbial compositions and the different culture conditions revealed that in 25% NaCl, the samples did not differ significantly based on the incubation period, but the concentration of phosphate resulted in a small difference between the samples (Fig. S1). On the other hand, in 15% NaCl the samples were separated according to both the phosphate concentration and incubation time (Fig. S1).

In accordance with the alpha diversity results, NaCl concentration was a key parameter in determining the species apparently selected under each condition. At 15% NaCl, 16S sequences associated with Bacteroidetes and Proteobacteria are the most abundant after 30 days of incubation (Fig. 3a). The phosphate concentration did not substantially affect the microbial composition in 15% NaCl at the phylum level, and the presence of Euryarchaeota 16S sequences was found at very low levels (Fig. 3a).

On the other hand, in 25% NaCl, the relative abundance of Euryarchaeota 16S sequences was much higher and increased over time (Fig. 3a). At this NaCl concentration, the phosphate presence notably affected the community composition, since without phosphate on day 30, the microbial diversity determined by the relative abundance of 16S sequences was mainly composed of Euryarchaeota (ca. 50%) and Bacteroidetes (ca. 37.5%), while in the presence of 1 mM phosphate at the end of the incubation, Euryarchaeota (ca. 40%) and Proteobacteria (ca. 40%) were the main phyla present (Fig. 3a).

At the genus level, in 15% NaCl, changes in microbial diversity were observed between day 7 and day 15 under both phosphate conditions (Fig. 3b). The relative abundance of *Sediminimonas* increased from ca. 20−35% to more than 50%, turning into the predominant genus independently of the presence of phosphate during incubation. At 15% NaCl, in presence of 1 mM phosphate, the *Idiomarina*, *Halomonas*,

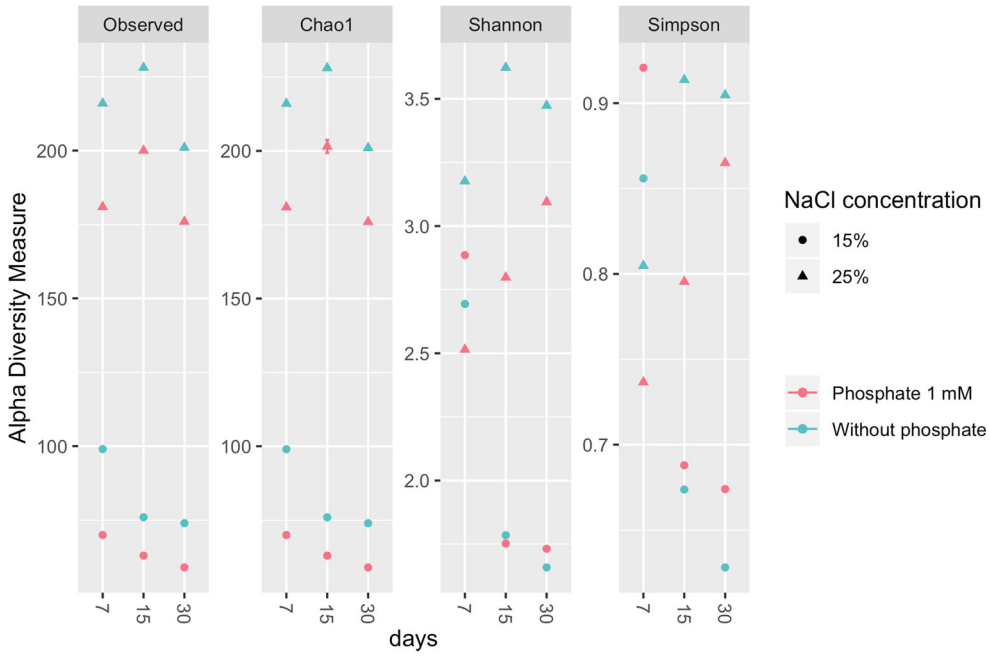

Fig. 2 Observed, Chao1, Shannon, and Simpson alpha diversity measures of selective cultures under different incubation conditions

and *Halorubrum* genera, which were abundant members of the community on day 7, were not detected at days 15 and 30. At the end of incubation, the microbial community was composed mainly of *Sediminimonas*, *Salisaeta*, and *Psychroflexus*. The same occurred without the phosphate addition in culture medium with 15% NaCl, where *Salinibacter* and *Halomonas* radically decreased their abundance in the samples on days 15 and 30 of incubation, leaving the enrichment culture dominated by *Sediminimonas*, *Salisaeta*, and *Psychroflexus*.

Also, at 25% NaCl, a gradual change in the relative abundance of the different genera was observed over time in the presence or absence of phosphate (Fig. 3b). When 1 mM phosphate was added to the culture medium, the microbial diversity on day 7, composed mainly of *Salicola* (75% approx.) and *Halorubrum* (15% approx.) genera, changed over the incubation period, with *Halorubrum* relative abundance reaching ca. 37.5% at day 30. At this time point, the relative abundance of *Salicola* decreased to only about 40%. In the absence of phosphate, a similar behavior of *Halorubrum* was observed. Additionally, the relative abundance of the dominant bacterial genus *Salinibacter* decreased to ca. 37.5 % over time (Fig. 3b).

The data of the functional analysis obtained by PICRUSt2, and statistical analyses by STAMP, revealed significant differences between the samples treated with 15% and 25% NaCl (Fig. 4). At a lower salinity (15 % NaCl), the *acr3*, *arsC1*, *arsC2*, *phoB*, and *phoR* genes were predicted to be more abundant when compared to 25% NaCl. In contrast, in samples incubated with 25% NaCl, genes belonging to the *pstSCAB-phoU* operon and *arsA* were predicted in more abundant percentages. Phosphate concentration only affected the prediction of gene abundance in the samples treated with 25% NaCl: the *arsC1* and *pstS* genes were more abundant within 1 mM phosphate present in the medium, while *arsC2* were predicted to be more abundant when no phosphate was added (Fig. S2). The *aioAB* genes and *arrAB* genes were not detected in significant abundances in any condition. The analyzed genes did not show significant differences between the evaluated days.

Experiments with *Halorubrum* sp. and *Salicola* sp. Isolates

The microbial mat from Laguna Tebenquiche was incubated for 7 days in CDM culture medium supplemented with 20% NaCl, 25 mM arsenate, and no addition of phosphate. Then, the enrichments were streaked onto CDM medium agar plates (see "Methods" section). After 5 days of incubation on plates, two isolates were obtained with 20% NaCl, 25 mM arsenate, and no phosphate addition to the culture medium. The isolates had distinct pigmentation, one being red and the other one whitish. 16s rRNA gene sequencing showed that the red-pigmented isolate corresponded to *Halorubrum* sp. (strain TLS-6), while the whitish isolate corresponded to *Salicola* sp. (strain TLS-7). These two genera were also detected as the dominant species in our 25% NaCl enrichments (Fig. 3). Thus, these isolates represent a successful isolation of endemic microorganisms of AMEs in the Laguna Tebenquiche.

The isolated strains were physiologically characterized, and both showed aerobic metabolism and the capacity to grow in the presence of high arsenate concentration even under no added inorganic phosphate conditions (3 μM according to

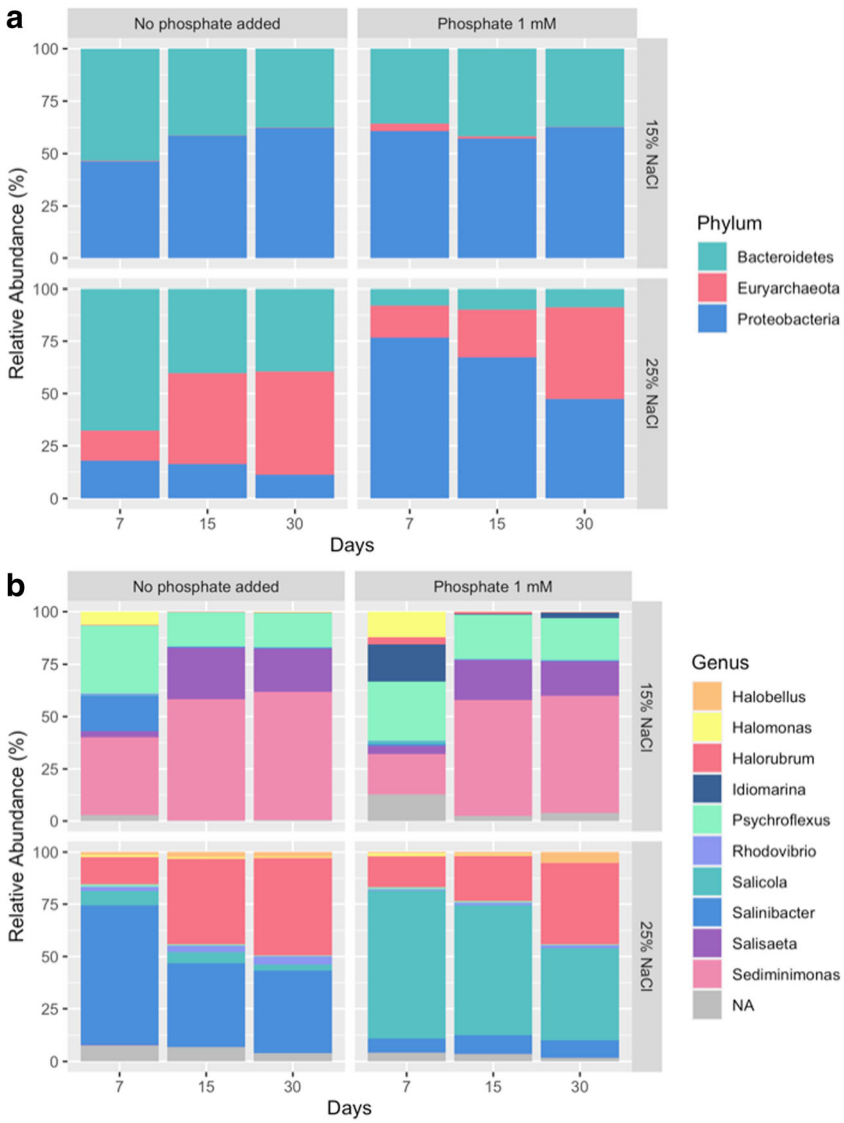

Fig. 3 Microbial mat biodiversity in culture media supplemented with 15% and 25% NaCl. Samples (no phosphate added and phosphate 1 mM) were incubated for 30 days and aliquots were taken at 7, 15, and 30 days and were used for DNA extraction. The taxonomic level graphed was phylum (**a**) and genus (**b**)

ICP-MS quantification, Fig. S3). The low phosphate conditions strongly decreased the growth of both isolates, but in *Halorubrum* sp. TLS-6 increasing the arsenate concentration showed a positive effect on growth under this condition (Fig. S3). A similar arsenotrophic behavior for the strain *Halorubrum sp.* DM2 isolated from Laguna Diamante was previously reported [19]. The same effect was not observed with the bacterial isolate *Salicola* sp. TLS-7.

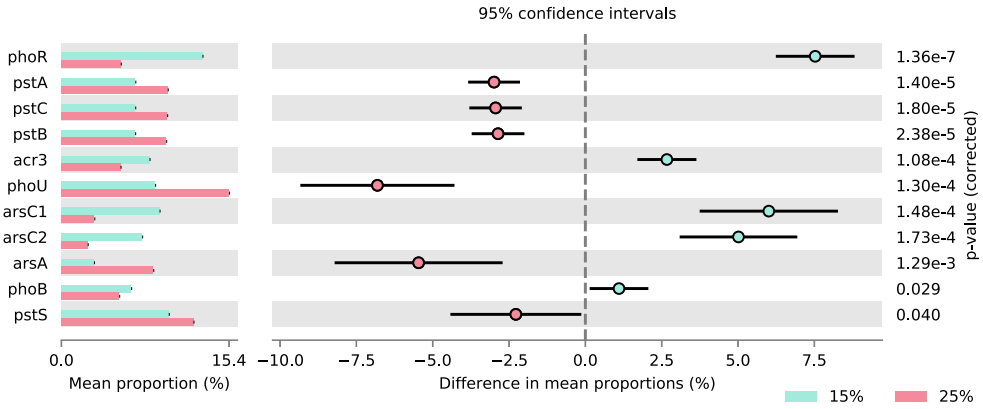

Fig. 4 PICRUSt 2 function analysis. Predicted functional subsystems at KEEG Orthology (KO) database with a significantly different ($p < 0.05$) between 15 and 25% NaCl concentration samples using *t* test (equal variance) as a statistical test in the STAMP software

Maximum growth rates for both isolates were observed at 1 mM phosphate and could tolerate high As concentration. No effect of As on the growth rate was observed (Fig. S3). In addition, neither isolate was completely growth-inhibited even in a medium supplemented with 500 mM As(V) (data not shown) (a higher concentration of As(V) in CDM medium was not possible to solubilize).

The analysis of the genomes of the TLS-6 and TLS-7 strains showed that all genes belonging to the specific phosphate transport system Pst are predicted to be present (Fig. 5). In the case of *Halorubrum* sp. TLS-6, the *pstSCAB-phoU* operon was complete; in addition, it also contained the gene for arsenate reductase *arsC2*. This is different from *Salicola* sp. TLS-7 *pstSCAB* genes, which are together without *phoU*. In *Salicola* sp. TLS-7, the *phoU* gene was close to the *phoR* and *phoB* genes of the Pho regulon (Fig. 5). Regarding the As-related genes, *aioAB* was not identified in Haloarchaea, but candidate *ars* and *acr* genes (*arsC2*, *arsA*, *arsD*, *arsR*, and *acr3*), which give resistance to the metalloid, were (Fig 4). *Salicola* sp. TLS-7 possesses candidate *aioAB* genes, which would allow obtaining energy by arsenite oxidation [18], as well as a candidate *arsH* organoarsenic oxidase gene, which confers As resistance in other species [18, 58].

Discussion

The presence of As across the microbial mat hints at a flow of As-rich water throughout the whole biomineral; the fact that As was clearly accumulated in discrete layers (Fig. 1) strongly suggests an active metabolic cycle related to As, which is consistent with the results obtained with the isolated microorganisms from the microbial mat. The biological role of As has been studied previously in other microbial ecosystems (in both lithifying and non-lithifying types) [19, 20, 31, 33, 59, 60] and even goes back to Archean ecosystems, where the use of As(III) for energy obtaining through photosynthesis has been proposed [29]. Recently, it was shown that arsenotrophic microbial mats from Laguna La Brava (also located in the Atacama Desert) are inhabited by populations of microorganisms that in energy terms preferably use arsenate reduction over sulfate reduction, making this ecosystem an excellent analog for primitive life [61]. The interaction of As with microbial ecosystems has been mainly studied in environments with a high As concentration such as Mono Lake and Searles Lake (0.2−3.0 mM) [33], Laguna Diamante (4.6 mM) [16, 20], and Laguna La Brava (0.8−1.5 mM) [12, 22, 61]. Although the As concentration in Laguna Tebenquiche is lower than in the lakes mentioned above (0.053 mM), we hypothesized that the metabolisms related to As in microbial

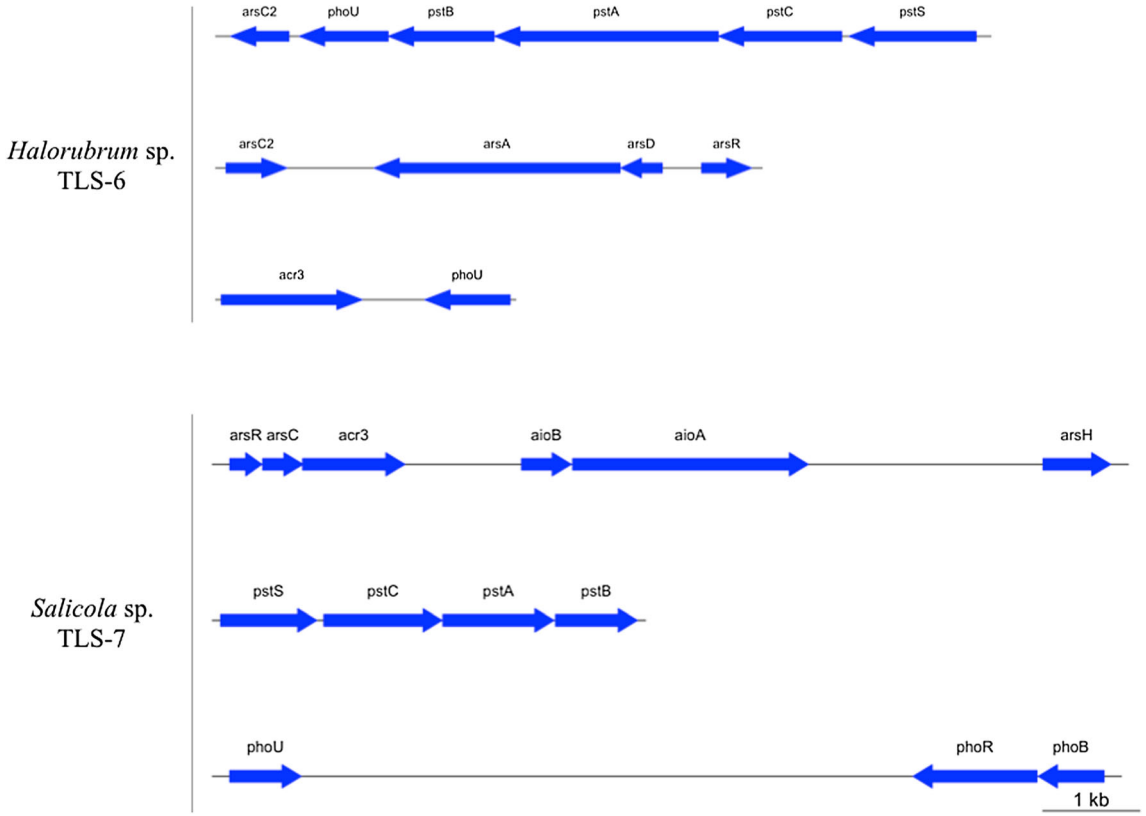

Fig. 5 Genomic organization of the genes related to both As and phosphate metabolism in *Halorubrum* sp. TLS-6 and in *Salicola* sp. TLS-7. Genes are scaled to their relative amino-acid sequence sizes. The gene map was created using the R package genoplotR [57]

ecosystems already described could also be present in the Laguna Tebenquiche. Moreover, the concentration of phosphate in the water column is even lower than that of As (0.011 mM), making it an ideal ecosystem to study the effect of low phosphate concentration on As metabolism, since the absence of sufficient phosphate could favor a higher As uptake by the microorganisms. As in, we have performed studies on whole mat sections; a next step might be to look layer by layer metagenomics studies to determine the abundance of functional genes related to As metabolism within the microbial communities.

Salinity is a key factor for understanding the biological role of As in extremophiles microbial communities [42, 59, 62] and has been studied in saline environments at different pH ranges [42, 63–65]. The salinity of Laguna Tebenquiche undergoes high changes both in space and time, ranging between 1 and 30% (w/v) [15]. These differences in the water column salinity have been associated with changes in microbial community composition [15]. Previous studies demonstrated a predominance of Bacteroidetes and Proteobacteria phyla, and particularly a high abundance of *Salinibacter* was found in the saltiest part of the lake [15]. Our results are in accordance with this, since the main factor that led to a change in microbial diversity of enriched cultures was the NaCl concentration (Fig. 3a). Just as in the natural environment, *Salinibacter* is the dominant genus in the saltiest condition (25% NaCl), but only when phosphate was not added (Fig. 3b). Proteobacteria and Bacteroidetes were also the dominant phyla present in the samples with 15% NaCl (Fig. 3a). Proteobacteria were mostly represented by the genus *Sediminimonas* (alpha-Proteobacteria) which has been previously reported in salt mines and saline soils [66, 67], and to a lesser extent *Idiomarina* (Gammaproteobacteria). Both genera have been described as being part of lithifying and non-lithifying hypersaline microbial mats [55, 68], and Idiomarina was also reported to contain copies of the *arsC* gene [55, 69].

Our results do not suggest that phosphate concentration affects microbial diversity in 15% NaCl (Fig. 2; Fig. 3), whereas it seems to have an effect on 25% NaCl, a condition where the relative abundance of archaea in the culture increased over time, reaching more than 35% (Fig. 3). The presence of phosphate (in 25% NaCl) favored the abundance of Proteobacteria, while without the addition of phosphate to the medium, Bacteroidetes were favored, specifically the genus *Salinibacter* (Fig. 3b). *Salinibacter* is an extremely halophilic bacterium that has been studied for having archaeal-like properties [70–72]. These studies have concluded that although phylogenetically *Salinibacter* belongs to Bacteroidetes, physiologically it behaves like an archaeon and they also commonly share habitats. It is presumed that different sets of genes have been shared by lateral transfer from archaea to *Salinibacter* [70, 71, 73], impacting the physiology of the bacterium and its adaptation to stress conditions such as high salinity and high UV radiation, among others [70]. It is therefore interesting that in our 25% NaCl incubation, the enriched culture of the microbial mat was strongly dominated by *Halorubrum* and *Salinibacter* (Fig. 3b). However, this was only observed when phosphate was not added to the culture medium, suggesting that under low phosphate concentration archaea are better adapted to those conditions. In the presence of phosphate (under 25% NaCl), the genus *Salicola* exhibited the highest relative abundance. *Salicola* is a halophilic bacterium that, together with *Salinibacter*, usually dominates extremely saline water bodies that are around halite saturation [74].

In addition to the switch from Proteobacteria to Bacteroidetes that occurred in 25% NaCl depending on phosphate concentration, the most striking observation in high salinity incubations was the presence of Euryarchaeota, specifically *Halorubrum*, a widely distributed halophilic archaeon in AMEs (Fig. 3). Its relative abundance increased over incubation time in both phosphate conditions (in 25% NaCl) and although it was little affected by the phosphate concentration, *Halorubrum* was more abundant when no phosphate was added (Fig. 3a).

From the taxonomic diversity, PICRUSt2 results revealed that the NaCl concentration was the main parameter responsible for the observed differences in predicted gene abundance. This is in agreement since the prediction of genes is made from 16S sequences, and the NaCl concentration was the main parameter influencing changes in predicted microbial diversity (Fig. 3). The *pstSCAB-phoU* operon genes were predicted to be more abundant in the 25% NaCl condition—where there would be a strong dominance of archaea—suggesting that the genes for phosphate transport and homeostasis would be more widespread in archaea living under As stress. The genes of the *pstSCAB* operon in many cases sit together with the *phoU* gene that codes for an essential protein in P homeostasis, acting on the Pho regulon especially at high phosphate concentrations [75–77]. Previous metagenomic studies have suggested that the red biofilm that inhabits the Laguna Diamante, characterized by strong dominance of archaea (94%) [20] and high As concentrations (up to 347 mg/L in summer) [16], has a high abundance of putative *pstSCAB-phoU* operon genes compared to other AMEs [41]. On the other hand, incubation time did not significantly influence predicted gene abundance, whereas phosphate concentration influenced the abundance prediction of a few genes—*arsC1*, *arsC2*, and *pstS*—but only when the NaCl concentration was 25% (Fig. S2). *arsC1* and *pstS* were predicted to be more abundant in the presence of phosphate while the *arsC2* would be more abundant without phosphate. *arsC1* and *arsC2* code for arsenate reductases related to the mycothiol-dependent class and thioredoxin reductase-dependent class, respectively [78]. These results could indicate that in low phosphate concentration where

Halorubrum and *Salinibacter* would be more abundant (Fig. 3b), the *arsC2* gene prediction is prevalent. In contrast, under 1 mM phosphate the *arsC1* gene would be more abundant, suggesting that it could be part of the *Salicola* genome. Our analysis of the *Salicola* sp. TLS-7 strain genome confirmed the presence of the *arsC1* gene (Fig. 5). These predictions present new hypotheses to further test with more powerful methods such as metagenomics and metatranscriptomics.

The physical proximity between the genes related to As metabolism and the *pstSCAB-phoU* operon that we observed in our genomes (Fig. 5) has been previously described [79]. These genomic regions where *aioAB* genes are clustered together with other genes related to As resistance and phosphate metabolism have been named "arsenic islands" [18, 79]. Here, we have shown the genome analysis of two endemic microorganisms (*Halorubrum* and *Salicola*) inhabiting microbial mat from Laguna Tebenquiche. The genome of the *Salicola* isolate represents the first whole genome published of this genus. The *Salicola* sp. TLS-7 genome includes As resistance genes and for obtaining energy from As transformations (*aioAB*); although candidate genes for the Pst-PhoU system were also present, they were not found in the same genomic context. In contrast, in *Halorubrum* sp. TLS-6 the *arsC2* gene was found together with the Pst-PhoU transport system and additionally, it contained a second copy of *phoU*, which was located next to the *acr3* gene, suggesting a more specific relationship. Although the phosphate-arsenic relationship has been studied at the physiological level, in the genomic context, it is still unknown and suggests cooperation so that cells can obtain the small amount of phosphate that they need in the context of high As concentration [41, 79, 80].

Our results describe the phosphate-As interactions with the microbial mat that inhabit the Laguna Tebenquiche. Here, As is present not only in the water column but is distributed throughout the microbial mat in an environment where the phosphate concentration is not very high (0.011 mM [41]; Fig. 1). We saw that changing phosphate concentration drastically altered the taxonomic composition of the enriched cultures under 25% NaCl, conditions in which archaea played a preponderant role (Fig. 3). Under 25% NaCl (a condition with high relative abundance of archaea), the genes of the Pst system were predicted to be more abundant than under 15% NaCl (Fig. 4). Finally, in the *Halorubrum* sp. TLS-6 isolate, the genes of the Pst system were found next to the arsenate reductase gene (*arsC2*) and the *phoU* gene together with the *acr3* transporter (Fig. 5). All these results suggest a tight phosphate-arsenic relationship in the hypersaline microbial mat from Laguna Tebenquiche.

Supplementary Information The online version contains supplementary material available at https://doi.org/10.1007/s00248-020-01673-9.

Acknowledgments We are very grateful to Dr. Heidi Taubner from MARUM - AG Hinrichs (Bremen University) for her help and time in using the μ-XRF. LAS wants to acknowledge to German Academic Exchange Service (DAAD) for the financial assistance that has enabled him to perform a stay in MPI-Bremen with the supervision of Dr. Jana Milucka. MEF was funded by "PICT 3825 – CONICET." ECN was funded by "ANID-FONDECYT Regular 1200834" and by "ANID-PIA-Anillo INACH ACT192057." The μ-XRF system has been financed by the Deutsche Forschungsgemeinschaft with funds dedicated to the acquisition of large instrumentation granted to the University of Bremen in the framework of the Excellence Initiative.

Author Contribution Statement LAS contributed with the principal idea of this work, chose the study design, performed both the data analysis and the experiments, interpreted data, and wrote the paper. MS contributed to data analysis and assisted in writing the article. VDT participated in the study design, interpreted data, and substantively revised the manuscript. LW participated in the study design interpreted data and substantively revised the manuscript. JM participated in the study design and substantively revised the manuscript. ECN participated in the study design and contributed to the sequencing of genomes. CM contributed to the sequencing of genomes. MC obtained funding for the original project idea. MEF obtained funding for the original project idea, contributed to the work proposal, with the sampling and sequencing of the amplicons. All authors read and approved this manuscript.

Compliance with Ethical Standards

Conflict of Interest The authors declare that there is no conflict of interest.

References

1. Whittaker WR, Bapna D, Maimone MW, Rollins E (1997) Atacama Desert Trek: A Planetary Analog Filed Experiment. In: International Symposium on Artificial Intelligence, Robotics and Automation for Space (i-SAIRAS), pp 355–360
2. Saltern A, Lizama C, Monteoliva-Sa M et al (2002) Halorubrum tebenquichense sp. nov., a novel halophilic archaeon isolated from the Atacama Saltern. Chile. Int J Syst Evol Microbiol 52:149–155. https://doi.org/10.1099/00207713-52-1-149
3. Wierzchos J, Cámara B, De Los Ríos A et al (2011) Microbial colonization of Ca-sulfate crusts in the hyperarid core of the Atacama Desert: implications for the search for life on Mars. Geobiology 9:44–60. https://doi.org/10.1111/j.1472-4669.2010.00254.x
4. Wierzchos J, Ascaso C, McKay CP (2006) Endolithic cyanobacteria in halite rocks from the hyperarid core of the Atacama desert. Astrobiology 6:415–422
5. Connon SA, Lester ED, Shafaat HS et al (2007) Bacterial diversity in hyperarid Atacama Desert soils. J Geophys Res Biogeosci 112:n/a. https://doi.org/10.1029/2006JG000311
6. Garreaud RD, Molina A, Farias M (2010) Andean uplift, ocean cooling and Atacama hyperaridity: a climate modeling perspective. Earth Planet Sci Lett 292:39–50. https://doi.org/10.1016/J.EPSL.2010.01.017
7. Hartley AJ, Chong G, Houston J, Mather AE (2005) 150 million years of climatic stability: evidence from the Atacama Desert, northern Chile. J Geol Soc Lond 162:421–424. https://doi.org/10.1144/0016-764904-071
8. Risacher F, Alonso H, Salazar C (2003) The origin of brines and salts in Chilean salars: a hydrochemical review. Earth Sci Rev 63:249–293. https://doi.org/10.1016/S0012-8252(03)00037-0

9. Schulze-Makuch D, Wagner D, Kounaves SP, Mangelsdorf K, Devine KG, de Vera JP, Schmitt-Kopplin P, Grossart HP, Parro V, Kaupenjohann M, Galy A, Schneider B, Airo A, Frösler J, Davila AF, Arens FL, Cáceres L, Cornejo FS, Carrizo D, Dartnell L, DiRuggiero J, Flury M, Ganzert L, Gessner MO, Grathwohl P, Guan L, Heinz J, Hess M, Keppler F, Maus D, McKay CP, Meckenstock RU, Montgomery W, Oberlin EA, Probst AJ, Sáenz JS, Sattler T, Schirmack J, Sephton MA, Schloter M, Uhl J, Valenzuela B, Vestergaard G, Wörmer L, Zamorano P (2018) Transitory microbial habitat in the hyperarid Atacama Desert. Proc Natl Acad Sci U S A 115:2670–2675. https://doi.org/10.1073/pnas.1714341115
10. Fernandez AB, Rasuk MC, Visscher PT, Contreras M, Novoa F, Poire DG, Patterson MM, Ventosa A, Farias ME (2016) Microbial diversity in sediment ecosystems (evaporites domes, microbial mats, and crusts) of hypersaline Laguna Tebenquiche, Salar de Atacama, Chile. Front Microbiol 7:1284. https://doi.org/10.3389/fmicb.2016.01284
11. Escudero LV, Casamayor EO, Chong G, Pedrós-Alió C, Demergasso C (2013) Distribution of microbial arsenic reduction, oxidation and extrusion genes along a wide range of environmental arsenic concentrations. PLoS One 8:e78890. https://doi.org/10.1371/journal.pone.0078890
12. Farías ME, Rasuk MC, Gallagher KL et al (2017) Prokaryotic diversity and biogeochemical characteristics of benthic microbial ecosystems at La Brava, a hypersaline lake at Salar de Atacama, Chile. PLoS One 12:e0186867. https://doi.org/10.1371/journal.pone.0186867
13. Rasuk MC, Fernández AB, Kurth D, Contreras M, Novoa F, Poiré D, Farías ME (2016) Bacterial diversity in microbial mats and sediments from the Atacama Desert. Microb Ecol 71:44–56. https://doi.org/10.1007/s00248-015-0649-9
14. Demergasso C, Chong G, Galleguillos P et al (2003) Microbial mats from the Llamará salt flat, Northern Chile. Rev Chil Hist Nat 76:485–499
15. Demergasso C, Escudero L, Casamayor EO, Chong G, Balagué V, Pedrós-Alió C (2008) Novelty and spatio–temporal heterogeneity in the bacterial diversity of hypersaline Lake Tebenquiche (Salar de Atacama). Extremophiles 12:491–504
16. Saona Acuña LA, Soria MN, Villafañe PG, Stepanenko T, Farías ME (2020) Arsenic and Its Biological Role: From Early Earth to Current Andean Microbial Ecosystems. In: Farías M. (eds) Microbial Ecosystems in Central Andes Extreme Environments. Springer, Cham. https://doi.org/10.1007/978-3-030-36192-1_19
17. Farías ME, Rascovan N, Toneatti DM, Albarracín VH, Flores MR, Poiré DG, Collavino MM, Aguilar OM, Vazquez MP, Polerecky L (2013) The discovery of stromatolites developing at 3570 m above sea level in a high-altitude volcanic Lake Socompa, Argentinean Andes. PLoS One 8:e53497. https://doi.org/10.1371/journal.pone.0053497
18. Andres J, Bertin PN (2016) The microbial genomics of arsenic. FEMS Microbiol Rev 40:299–322. https://doi.org/10.1093/femsre/fuv050
19. Ordoñez OF, Rasuk MC, Soria MN et al (2018) Haloarchaea from the Andean Puna: biological role in the energy metabolism of arsenic. Microb Ecol 76:695–705. https://doi.org/10.1007/s00248-018-1159-3
20. Rascovan N, Maldonado J, Vazquez MP, Eugenia Farías M (2016) Metagenomic study of red biofilms from Diamante Lake reveals ancient arsenic bioenergetics in haloarchaea. ISME J 10:299–309. https://doi.org/10.1038/ismej.2015.109
21. Wang P, Sun G, Jia Y, Meharg AA, Zhu Y (2014) A review on completing arsenic biogeochemical cycle: microbial volatilization of arsines in environment. J Environ Sci (China) 26:371–381. https://doi.org/10.1016/S1001-0742(13)60432-5
22. Sancho-Tomás M, Somogyi A, Medjoubi K, Bergamaschi A, Visscher PT, van Driessche AES, Gérard E, Farias ME, Contreras M, Philippot P (2018) Distribution, redox state and (bio) geochemical implications of arsenic in present day microbialites of Laguna Brava, Salar de Atacama. Chem Geol 490:13–21. https://doi.org/10.1016/j.chemgeo.2018.04.029
23. Knodle R, Agarwal P, Brown M (2012) From phosphorous to arsenic: changing the classic paradigm for the structure of biomolecules. Biomolecules 2:282–287
24. Tawfik DS, Viola RE (2011) Arsenate replacing phosphate: alternative life CHEMISTRIES AND ION PROMISCUITY. Biochemistry 50:1128–1134. https://doi.org/10.1021/bi200002a
25. Tamaki S, Frankenberger WT (1992) Environmental biochemistry of arsenic. Rev Environ Contam Toxicol 124:79–110
26. Wurl O, Zimmer L, Cutter GA (2013) Arsenic and phosphorus biogeochemistry in the ocean: arsenic species as proxies for P-limitation. Limnol Oceanogr 58:729–740. https://doi.org/10.4319/lo.2013.58.2.0729
27. Guo P, Gong Y, Wang C, Liu X, Liu J (2011) Arsenic speciation and effect of arsenate inhibition in a Microcystis aeruginosa culture medium under different phosphate regimes. Environ Toxicol Chem 30:1754–1759. https://doi.org/10.1002/etc.567
28. Willsky GR, Malamy MH (1980) Effect of arsenate on inorganic phosphate transport in Escherichia coli. J Bacteriol 144:366–374
29. Sforna MC, Philippot P, Somogyi A, van Zuilen MA, Medjoubi K, Schoepp-Cothenet B, Nitschke W, Visscher PT (2014) Evidence for arsenic metabolism and cycling by microorganisms 2.7 billion years ago. Nat Geosci 7:811–815. https://doi.org/10.1038/ngeo2276
30. Kulp TR (2014) Arsenic and primordial life. Nat Geosci 7:785–786. https://doi.org/10.1038/ngeo2275
31. Kulp TR (2014) Early earth: arsenic and primordial life. Nat Geosci 7:785–786. https://doi.org/10.1038/ngeo2275
32. Lebrun E, Brugna M, Baymann F, Muller D, Lièvremont D, Lett MC, Nitschke W (2003) Arsenite oxidase, an ancient bioenergetic enzyme. Mol Biol Evol 20:686–693. https://doi.org/10.1093/molbev/msg071
33. Oremland RS, Saltikov CW, Wolfe-Simon F, Stolz JF (2009) Arsenic in the evolution of earth and extraterrestrial ecosystems. Geomicrobiol J 26:522–536. https://doi.org/10.1080/01490450903102525
34. Goldford JE, Hartman H, Smith TF, Segrè D (2017) Remnants of an Ancient metabolism without phosphate. Cell 168:1126–1134.e9. https://doi.org/10.1016/j.cell.2017.02.001
35. Pasek M (2019) A role for phosphorus redox in emerging and modern biochemistry. Curr Opin Chem Biol 49:53–58. https://doi.org/10.1016/J.CBPA.2018.09.018
36. Pasek MA (2008) Rethinking early Earth phosphorus geochemistry. Proc Natl Acad Sci U S A 105:853–858. https://doi.org/10.1073/pnas.0708205105
37. Ordoñez OF, Lanzarotti E, Kurth D et al (2015) Genome comparison of two Exiguobacterium strains from high altitude andean lakes with different arsenic resistance: identification and 3D modeling of the Acr3 efflux pump. Front Environ Sci 3. https://doi.org/10.3389/fenvs.2015.00050
38. Zannier F, Portero LR, Ordoñez OF et al (2019) Polyextremophilic bacteria from high altitude Andean Lakes: arsenic resistance profiles and biofilm production. Biomed Res Int 2019:1–11. https://doi.org/10.1155/2019/1231975
39. Castro-Severyn J, Remonsellez F, Valenzuela SL, Salinas C, Fortt J, Aguilar P, Pardo-Esté C, Dorador C, Quatrini R, Molina F, Aguayo D, Castro-Nallar E, Saavedra CP (2017) Comparative genomics analysis of a new Exiguobacterium strain from Salar de Huasco reveals a repertoire of stress-related genes and arsenic resistance. Front Microbiol 8:456. https://doi.org/10.3389/fmicb.2017.00456

40. Lizama C, Monteoliva-Sánchez M, Suárez-García A, Roselló-Mora R, Aguilera M, Campos V, Ramos-Cormenzana A (2002) Halorubrum tebenquichense sp. nov., a novel halophilic archaeon isolated from the Atacama Saltern, Chile. Int J Syst Evol Microbiol 52:149–155. https://doi.org/10.1099/00207713-52-1-149
41. Saona LA, Valenzuela-Diaz S, Kurth D et al (2019) Analysis of co-regulated abundance of genes associated with arsenic and phosphate metabolism in Andean Microbial Ecosystems. bioRxiv: 870428. https://doi.org/10.1101/870428
42. Lara J, Escudero González L, Ferrero M, Chong Díaz G, Pedrós-Alió C, Demergasso C (2012) Enrichment of arsenic transforming and resistant heterotrophic bacteria from sediments of two salt lakes in Northern Chile. Extremophiles 16:523–538. https://doi.org/10.1007/s00792-012-0452-1
43. Farías ME, Contreras M, Rasuk MC, Kurth D, Flores MR, Poiré DG, Novoa F, Visscher PT (2014) Characterization of bacterial diversity associated with microbial mats, gypsum evaporites and carbonate microbialites in thalassic wetlands: Tebenquiche and La Brava, Salar de Atacama, Chile. Extremophiles 18:311–329
44. Kauri T, Wallace R, Kushner DJ (1990) Nutrition of the Halophilic Archaebacterium, Haloferax volcanii. Syst Appl Microbiol 13:14–18. https://doi.org/10.1016/S0723-2020(11)80174-8
45. Klindworth A, Pruesse E, Schweer T, Peplies J, Quast C, Horn M, Glöckner FO (2013) Evaluation of general 16S ribosomal RNA gene PCR primers for classical and next-generation sequencing-based diversity studies. Nucleic Acids Res 41:e1
46. Raskin L, Stromley JM, Rittmann BE, Stahll' DA, (1994) Group-specific 16S rRNA hybridization probes to describe natural communities of methanogens. Appl Environ Microbiol 60(4):1232–1240
47. Heuer H, Krsek M, Baker P, Smalla K, Wellington EM (1997) Analysis of actinomycete communities by specific amplification of genes encoding 16S rRNA and gel-electrophoretic separation in denaturing gradients. Appl Environ Microbiol 63:3233–3241. https://doi.org/10.1128/aem.63.8.3233-3241.1997
48. Altschul SF, Gish W, Miller W, Myers EW, Lipman DJ (1990) Basic local alignment search tool. J Mol Biol 215:403–410. https://doi.org/10.1016/S0022-2836(05)80360-2
49. Callahan BJ, McMurdie PJ, Rosen MJ et al (2016) DADA2: high-resolution sample inference from Illumina amplicon data. Nat Methods 13:581–583. https://doi.org/10.1038/nmeth.3869
50. Quast C, Pruesse E, Yilmaz P, Gerken J, Schweer T, Yarza P, Peplies J, Glöckner FO (2012) The SILVA ribosomal RNA gene database project: improved data processing and web-based tools. Nucleic Acids Res 41:D590–D596. https://doi.org/10.1093/nar/gks1219
51. McMurdie PJ, Holmes S (2013) phyloseq: An R package for reproducible Interactive analysis and graphics of microbiome census data. PLoS One 8:e61217. https://doi.org/10.1371/journal.pone.0061217
52. Langille MGI, Zaneveld J, Caporaso JG, McDonald D, Knights D, Reyes JA, Clemente JC, Burkepile DE, Vega Thurber RL, Knight R, Beiko RG, Huttenhower C (2013) Predictive functional profiling of microbial communities using 16S rRNA marker gene sequences. Nat Biotechnol 31:814–821. https://doi.org/10.1038/nbt.2676
53. Wu J, Peters BA, Dominianni C, Zhang Y, Pei Z, Yang L, Ma Y, Purdue MP, Jacobs EJ, Gapstur SM, Li H, Alekseyenko AV, Hayes RB, Ahn J (2016) Cigarette smoking and the oral microbiome in a large study of American adults. ISME J 10:2435–2446. https://doi.org/10.1038/ismej.2016.37
54. Parks DH, Tyson GW, Hugenholtz P, Beiko RG (2014) STAMP: statistical analysis of taxonomic and functional profiles. Bioinformatics 30:3123–3124. https://doi.org/10.1093/bioinformatics/btu494
55. Kurth D, Amadio A, Ordoñez OF et al (2017) Arsenic metabolism in high altitude modern stromatolites revealed by metagenomic analysis. Sci Rep 7:1024. https://doi.org/10.1038/s41598-017-00896-0
56. R Development Core Team R (2012) A language and environment for statistical computing. R Foundation for Statistical Computing, Vienna
57. Guy L, Roat Kultima J, Andersson SGE (2010) genoPlotR: comparative gene and genome visualization in R. Bioinformatics 26: 2334–2335. https://doi.org/10.1093/bioinformatics/btq413
58. Chen J, Bhattacharjee H, Rosen BP (2015) ArsH is an organoarsenical oxidase that confers resistance to trivalent forms of the herbicide monosodium methylarsenate and the poultry growth promoter roxarsone. Mol Microbiol 96:1042–1052. https://doi.org/10.1111/mmi.12988
59. Price RE, Lesniewski R, Nitzsche KS, Meyerdierks A, Saltikov C, Pichler T, Amend JP (2013) Archaeal and bacterial diversity in an arsenic-rich shallow-sea hydrothermal system undergoing phase separation. Front Microbiol 4:158. https://doi.org/10.3389/fmicb.2013.00158
60. Hoeft SE, Kulp TR, Han S, Lanoil B, Oremland RS (2010) Coupled arsenotrophy in a hot spring photosynthetic biofilm at mono lake, california. Appl Environ Microbiol 76:4633–4639. https://doi.org/10.1128/AEM.00545-10
61. Visscher PT, Gallagher KL, Bouton A, Farias ME, Kurth D, Sancho-Tomás M, Philippot P, Somogyi A, Medjoubi K, Vennin E, Bourillot R, Walter MR, Burns BP, Contreras M, Dupraz C (2020) Modern arsenotrophic microbial mats provide an analogue for life in the anoxic Archean. Commun Earth Environ 1:24. https://doi.org/10.1038/s43247-020-00025-2
62. Kulp TR, Han S, Saltikov CW, Lanoil BD, Zargar K, Oremland RS (2007) Effects of imposed salinity gradients on dissimilatory arsenate reduction, sulfate reduction, and other microbial processes in sediments from two California soda lakes. Appl Environ Microbiol 73:5130–5137. https://doi.org/10.1128/AEM.00771-07
63. Kulp TR, Hoeft SE, Asao M et al (2008) Arsenic (III) fuels anoxygenic photosynthesis in hot spring biofilms from Mono Lake, California. Science (80-) 321:967–970
64. Oremland RS, Stolz JF, Hollibaugh JT (2004) The microbial arsenic cycle in Mono Lake, California. FEMS Microbiol Ecol 48:15–27
65. Demergasso CS, Guillermo CD, Lorena EG, Mur JJP, Pedrós-Alió C (2007) Microbial precipitation of arsenic sulfides in Andean salt flats. Geomicrobiol J 24:111–123. https://doi.org/10.1080/01490450701266605
66. Wang YX, Wang ZG, Liu JH, Chen YG, Zhang XX, Wen ML, Xu LH, Peng Q, Cui XL (2009) Sediminimonas qiaohouensis gen. nov., sp. nov., a member of the Roseobacter clade in the order Rhodobacterales. Int J Syst Evol Microbiol 59:1561–1567. https://doi.org/10.1099/ijs.0.006965-0
67. Sen U, Mukhopadhyay SK (2019) Microbial community composition of saltern soils from Ramnagar, West Bengal, India. Ecol Genet Genomics 12:100040. https://doi.org/10.1016/j.egg.2019.100040
68. Schneider D, Arp G, Reimer A, Reitner J, Daniel R (2013) Phylogenetic analysis of a microbialite-forming microbial mat from a hypersaline lake of the Kiritimati Atoll, Central Pacific. PLoS One 8:e66662. https://doi.org/10.1371/journal.pone.0066662
69. Sinha RK, Krishnan KP, Kurian PJ (2017) Draft genome sequence of Idiomarina sp. strain 5.13, a highly stress-resistant bacterium isolated from the Southwest Indian Ridge. https://doi.org/10.1128/genomeA.01747-16
70. Oren A (2013) *Salinibacter* : an extremely halophilic bacterium with archaeal properties. FEMS Microbiol Lett 342:1–9. https://doi.org/10.1111/1574-6968.12094
71. Oren A, Rodríguez-Valera F, Antón J, Benlloch S, Rosselló-Mora R, Amann R, Coleman J, Russell NJ (2004) Red, Extremely Halophilic, but not Archaeal: The Physiology and Ecology of Salinibacter ruber, a Bacterium Isolated from Saltern Crystallizer

Ponds. In: Ventosa A. (eds) Halophilic Microorganisms. Springer, Berlin, Heidelberg. https://doi.org/10.1007/978-3-662-07656-9_4

72. Antón J, Peña A, Valens M, Santos F, Glöckner FO, Bauer M, Dopazo J, Herrero J, Rosselló-Mora R, Amann R (2005) Salinibacter Ruber: Genomics and Biogeography. In: Gunde-Cimerman N., Oren A., Plemenitaš A. (eds) Adaptation to Life at High Salt Concentrations in Archaea, Bacteria, and Eukarya. Cellular Origin, Life in Extreme Habitats and Astrobiology, vol 9. Springer, Dordrecht. https://doi.org/10.1007/1-4020-3633-7_17
73. Mongodin EF, Nelson KE, Daugherty S, DeBoy RT, Wister J, Khouri H, Weidman J, Walsh DA, Papke RT, Sanchez Perez G, Sharma AK, Nesbo CL, MacLeod D, Bapteste E, Doolittle WF, Charlebois RL, Legault B, Rodriguez-Valera F (2005) The genome of Salinibacter ruber: convergence and gene exchange among hyperhalophilic bacteria and archaea. Proc Natl Acad Sci U S A 102:18147–18152. https://doi.org/10.1073/pnas.0509073102
74. Nercessian D, Di Meglio L, De Castro R, Paggi R (2015) Exploring the multiple biotechnological potential of halophilic microorganisms isolated from two Argentinean salterns. Extremophiles 19: 1133–1143. https://doi.org/10.1007/s00792-015-0785-7
75. Vuppada RK, Hansen CR, Strickland KAP, Kelly KM, McCleary WR (2018) Phosphate signaling through alternate conformations of the PstSCAB phosphate transporter. BMC Microbiol 18:8. https://doi.org/10.1186/s12866-017-1126-z
76. Steed PM, Wanner BL (1993) Use of the rep technique for allele replacement to construct mutants with deletions of the pstSCAB-phoU operon: evidence of a new role for the PhoU protein in the phosphate regulon. J Bacteriol 175:6797–6809
77. Lamarche MG, Wanner BL, Crépin S, Harel J (2008) The phosphate regulon and bacterial virulence: a regulatory network connecting phosphate homeostasis and pathogenesis. FEMS Microbiol Rev 32:461–473. https://doi.org/10.1111/j.1574-6976.2008.00101.x
78. Firrincieli A, Presentato A, Favoino G, Marabottini R, Allevato E, Stazi SR, Scarascia Mugnozza G, Harfouche A, Petruccioli M, Turner RJ, Zannoni D, Cappelletti M (2019) Identification of resistance genes and response to arsenic in rhodococcus aetherivorans BCP1. Front Microbiol 10. https://doi.org/10.3389/fmicb.2019.00888
79. Li H, Li M, Huang Y, Rensing C, Wang G (2013) In silico analysis of bacterial arsenic islands reveals remarkable synteny and functional relatedness between arsenate and phosphate. Front Microbiol 4:347. https://doi.org/10.3389/fmicb.2013.00347
80. Schoepp-Cothenet B, Nitschke W, Barge LM, Ponce A, Russell MJ, Tsapin AI (2011) Comment on "A bacterium that can grow by using arsenic instead of phosphorus". Science 332:1149; author reply 1149. https://doi.org/10.1126/science.1201438